AFRL-AFOSR-CL-TR-2019-0008

Solar Flare Emissions from GHz to THz Frequencies

Jean-Pierre Raulin
INSTITUTO PRESBITERIANO MACKENZIE.
RUA DA CONSOLACAO 896
SAO PAULO, 01302-907
BR

05/02/2019
Final Report

Air Force Research Laboratory
Air Force Office of Scientific Research
Southern Office of Aerospace Research and Development
U.S. Embassy Santiago, AV. Andrews Bello 2800 Santiago, Chile

REPORT DOCUMENTATION PAGE

Form Approved
OMB No. 0704-0188

1. REPORT DATE *(DD-MM-YYYY)*	2. REPORT TYPE	3. DATES COVERED *(From - To)*
02-05-2019	Final	15 Jan 2016 to 14 Jan 2019

4. TITLE AND SUBTITLE
Solar Flare Emissions from GHz to THz Frequencies

5a. CONTRACT NUMBER

5b. GRANT NUMBER
FA9550-16-1-0072

5c. PROGRAM ELEMENT NUMBER
61102F

6. AUTHOR(S)
Jean-Pierre Raulin

5d. PROJECT NUMBER

5e. TASK NUMBER

5f. WORK UNIT NUMBER

7. PERFORMING ORGANIZATION NAME(S) AND ADDRESS(ES)
INSTITUTO PRESBITERIANO MACKENZIE.
RUA DA CONSOLACAO 896
SAO PAULO, 01302-907 BR

8. PERFORMING ORGANIZATION REPORT NUMBER

9. SPONSORING/MONITORING AGENCY NAME(S) AND ADDRESS(ES)
AFOSR/SOARD
U.S. Embassy Santiago
Av. Andres Bello 2800
Santiago, Chile

10. SPONSOR/MONITOR'S ACRONYM(S)
AFRL/AFOSR IOS

11. SPONSOR/MONITOR'S REPORT NUMBER(S)
AFRL-AFOSR-CL-TR-2019-0008

12. DISTRIBUTION/AVAILABILITY STATEMENT
A DISTRIBUTION UNLIMITED: PB Public Release

13. SUPPLEMENTARY NOTES

14. ABSTRACT
Despite the loss of former FA9550-16-1-0072 PI, Prof. P. Kaufmann, research activities and development went smoothly. FA9550-16-1-0072 brought important results on the atmospheric transmission through significant correlations between opacity measurements at 212 and 405 GHz, and PWV. Developments of new instrumental facilities at 30 THz and 16 THz (HATS), their installation, operation and exploration were successful. SOLAR-T stratospheric balloon experiment was well succeeded. Important results from solar flare emissions from microwaves to THz frequencies and mid-IR. The later appears has the low atmosphere response (heating) to energy deposit from precipitated accelerated particles.New insights on the role of secondary particles (electrons, knock-om electrons and positrons)during solar flares were obtained.

15. SUBJECT TERMS
Solar storms

16. SECURITY CLASSIFICATION OF:			17. LIMITATION OF ABSTRACT	18. NUMBER OF PAGES	19a. NAME OF RESPONSIBLE PERSON
a. REPORT	b. ABSTRACT	c. THIS PAGE			ANDERSEN, GEOFFREY
Unclassified	Unclassified	Unclassified	SAR		19b. TELEPHONE NUMBER *(Include area code)* 703-615-9465

SOLAR FLARE EMISSIONS FROM GHz TO THz FREQUENCIES

AFOSR Research Final Report

Grant Number FA9550-16-1-0072

Jean-Pierre Raulin, PI

This report was composed with the participation of the following Researchers and Students from CRAAM center: Jordi Tuneu, Daneele Tusnski, Sergio Szpigel, Adriana Valio, Douglas Silva, Carlos Giménez de Castro, Deysi Cornejo, Marta Cassiano, Ray Hidalgo, Emilia Correia, Pierre Kaufmann (in memoriam 1938-2017)

São Paulo, 04/2019

CONTENT

CONTEXT

This is the final report on Grant FA9550-16-1-0072 untitled *"Solar Flare Emission from GHz to THz Frequencies"*.

This report describes the main achievements as well as the scientific production in the form of published papers, invited reviews, and participation in national and international congresses.

We also remember the loss of Prof. Pierre Kaufmann in 2017, Feb. 17 at the initial stage of the project, former Principal Investigator of this AFOSR Grant.

REPORT

Initial Problem

The main problem to investigate in this project is to provide the observational diagnostic and perform the interpretation of solar explosive emission in a large frequency bandwidth from microwaves to 30 THz (10 microns, MIR). Over this ~ 5 decades frequency band, the spectral shape of solar flare emission is crucial to discuss the responsible processes as well as to provide constraints on the acceleration mechanism of particles like electrons and protons up to hundreds of Mev and few GeV, respectively.

In addition to the well-known microwave flare spectrum between few GHz and frequencies < 100 GHz, which is attributed to synchrotron radiation from middy-to-ultra-relativistic electrons, a new spectral component with flux densities increasing with frequency was discovered (Kaufmann et al., 2004).

The interpretation of this new component is not an easy task. It may represent the optically thick part of a new synchrotron spectrum peaking somewhere in the IR wavelength range from ultra-compact emitting sources to insure self-absorption of the emission below 100 GHz. An alternative was proposed by Kaufmann & Raulin (2006) where the emission at high frequencies results from incoherent synchrotron emission (ISR) from electron beams. In this approach, and depending on the physical properties of the particle beams, a microbunching instability can develop and produces coherent synchrotron radiation (CSR) at microwaves. The attractiveness of this scenario is that the extremely bright CSR is the product of a small fraction of particles within the initial beam. Therefore, such interpretation which provides naturally the presence of a double spectrum could bring important clues to solve the "electron number problem" which is often observed in microwaves during large solar flares. Some of the solar events showing increasing flux densities with frequency above 100 GHz, did also produce a hardening of the hard X-ray spectra above about 70 MeV. This is an early indication that the radio emission at high frequencies could include the synchrotron emission from positrons (Trottet et al., 2008). Indeed, during nuclear processes at work in solar flares, pions (π) can be produced. Neutral π^0 decay in 2 photons at ~ 70 MeV which produces the X-ray hardening, while charged π^+ and π^- decay to form electrons and positrons. These secondary particles will

radiate synchrotron fluxes which can add to that emission from primary electrons. More recently, and using new diagnostics in the IR wavelength range, the submillimeter flare emission was proposed to be the result of the chromospheric plasma response to the precipitation of energetic particles (Kaufmann et al., 2013; Trottet et al., 2015).

To bring new clues to the still open questions listed above, a detailed description of the solar flare spectra is needed within the GHz-to-THz frequency range. For this the CRAAM operates a 7 GHz solar polarimeter installed at the CRAAM center in São Paulo, UPM. Since 2012, CRAAM is also operating 45 and 90 GHz solar polarimeters to complement the flare spectra between microwaves and submillimeter waves. The Solar Submillimeter Telescope (SST) is providing continuous solar observations at 212 and 405 GHz, since 2000. More recently, 30 THz (10 microns) observations simultaneously obtained with H-α records are available in Brazil (at CRAAM center) and in Argentina (at OAFA observatory). In 2016, CRAAM flew the SOLAR-T module onboard a stratospheric balloon along with GRIPS experiment. SOLAR-T operated at 3 and 7 THz and brought very good results on the quiescent and transient solar emission at these two frequencies.

All the models discussed above assume flux densities radiated by the solar sources, free of any attenuation in the Earth atmosphere. This means that a special effort is also needed to understand the processes of absorption of very high frequency waves to estimate correct attenuation factors and provide reliable flux density values.

Conditions of observations at submillimeter wavelengths

Solar flare spectra can provide important information about the physical processes involved during flares, radiation mechanisms and to constraint mechanism of acceleration of particles. Observations at mm and submm wavelengths depend critically on atmospheric transparency, which becomes one important source of imprecision in the determination of brightness temperatures and fluxes at such frequencies. In turn, the atmospheric transmission is affected mainly by water vapor absorption.

For these reasons, an important effort was made in this project to study the atmospheric transparency.

Three methods were used. The chosen method, the "solar brightness" method (Melo et al., 2005), depends on the product P, of an efficiency term, η, and the brightness temperature of the Sun, T_S

Even though these parameters are not known with precision, their product P should be constant. Therefore, a mean value for P was determined for each beam of the SST during a 6 years period, only for transparent days with opacity determined by the "tipping" method. Once know the mean P, the atmospheric transmission was recalculated using the "solar brightness" method.

The 3 main results obtained, and summarized below were related to: (i) relation between τ_{212} and τ_{405} ; (ii) relation between submillimeter opacity and Precipitable Water Vapor

(PWV) ; (iii) PWV scale height. A detailed description of these results ae available in the two first progress reports.

Relation between τ_{212} and τ_{405}.

We find that a clear seasonal variation with mean values for opacity of 0.31 ± 0.06 and 2.2 ± 0.4 at 212 and 405 GHz, respectively, for the summer months and 0.16 ± 0.01 and 1.2 ± 0.13, respectively, for the winter months.

We also evidence a good correlation between the simultaneous measures of τ_{212} and τ_{405} for the CASLEO site as illustrated in Figure 1. Opacities at 405 GHz are 7 times greater than the opacities at 212 GHz. Therefore, this relation allows to estimate the opacity at 405 GHz, even when the sky is opaque at this frequency.

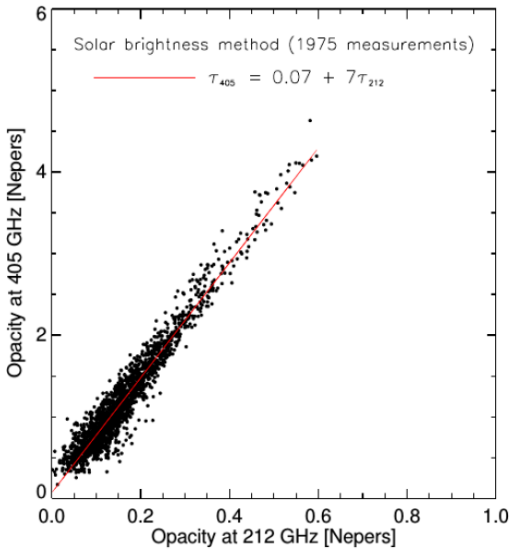

Figure 1: Correlation between τ_{212} and τ_{405} from the brightness method. The red line shows the best fit to the observed points.

Relation with Precipitable Water Vapor (PWV) measurements:

In the analysis of the correlation between PWV and 212 GHz atmospheric optical depth at El Leoncito, a dataset obtained simultaneously by SST and AERONET CASLEO station was used. The SST 212 GHz optical depths (τ_{212}) were derived as explained in the previous section. PWV Level 2.0 data, the highest data quality level provided by AERONET (Smirnov et al., 2000) were downloaded directly from the AERONET website. Radio and PWV measurements were obtained by less than 10 minutes apart, during clear sky conditions.

The correlation plot between the PWV and the optical depth τ_{212}, for the whole period of 2011–2013, is shown in Figure 2a. A very significant correlation was found by a linear fit, with a correlation coefficient of 0.98, that can be expressed as

$$\mathrm{PWV} = (14.3 \pm 0.2)\,\tau_{212} + (0.07 \pm 0.06)$$

with PWV given in mm, and τ_{212} in Nepers.

The data were also analyzed year by year and similar correlations were found. The values of the parameters obtained by linear fits are presented in Fig. 2b-d. The slope values of all fits, by considering the errors, are in the range of 13.5-14.9 mm/Np.

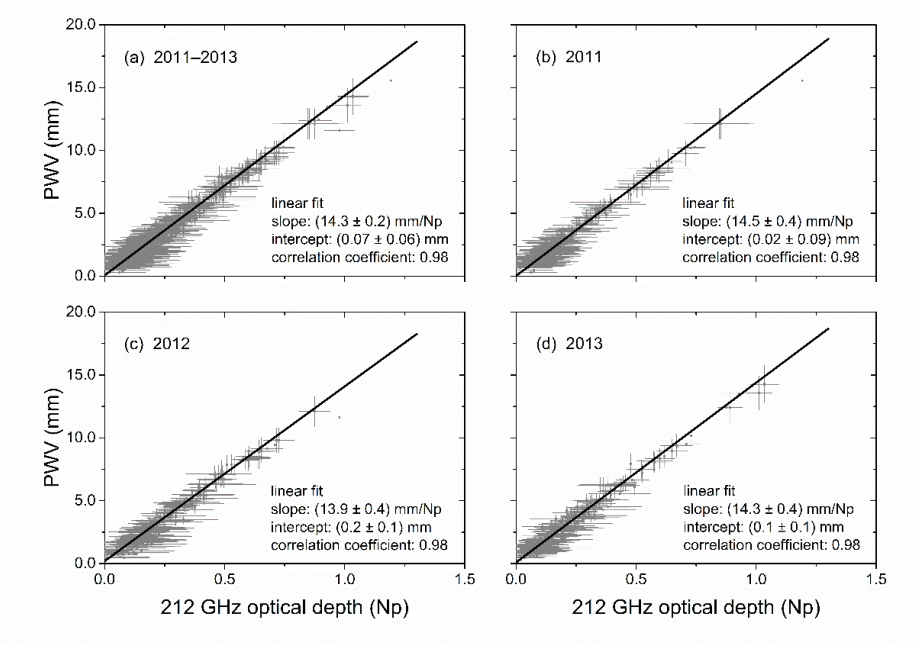

Figure 2. Precipitable water vapor and 212 GHz atmospheric optical depth correlation, at El Leoncito, for the whole period 2011–2013 (a) and for the years 2011 (b), 2012 (c), and 2013 (d). The values of the parameters obtained by linear fit are presented in each case (a)-(d).

Figure 3 shows the correlation plot between the PWV and the atmospheric optical depth τ_{405}. The very significant correlation, found by a linear fit, with a correlation coefficient of 0.99, can be expressed as

$$\mathrm{PWV} = (2.09 \pm 0.03)\,\tau_{405} + (-0.11 \pm 0.03)$$

with PWV in mm and τ_{405} in Nepers.

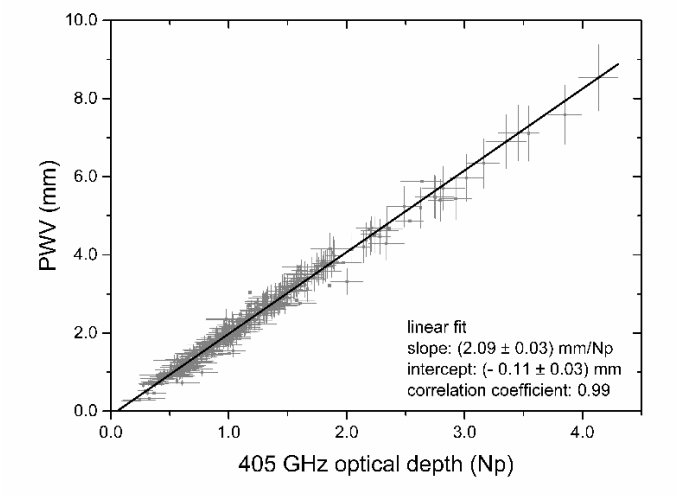

Figure 3. Precipitable water vapor and 405 GHz atmospheric optical depth correlation, at El Leoncito. The values of the parameters obtained by linear fit are presented in the plot.

SST data are available since 2002, which in principle allows the retrieval of optical depth values at 212 GHz from this epoch, using the above correlation. Such long-term PWV deduced time series can be a potentially valuable climate diagnostic for comparison with the solar cycle, Quasi Biennial Oscillations, El Niño phenomena, and other signatures of global climate changes.

PWV scale height:

The details of the atmospheric transmission model which would estimate the optical depth at high radio frequencies, like 212 GHz, from PWV measurements, can also be studied. The use of these models (Otarola et al., 2009; Otarola et al. 2010) generally end with a lower estimate of the millimeter and submillimeter optical depths compared to measurements. The reason deserves further study. However, a preliminary analysis (Figure 4) shows that agreement between PWV measurements and calculated values is obtained for a value of the PWV scale height of 1.3 km, different of that usually adopted of 2 km.

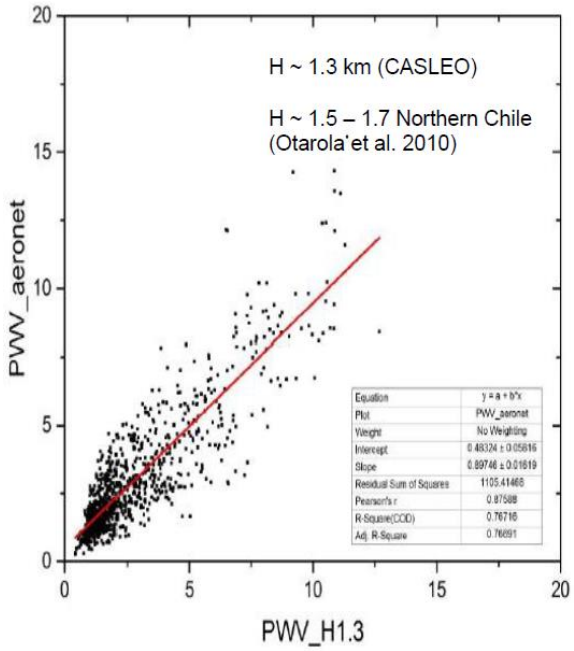

Figure 4. Comparison between calculated and observed precipitable water vapor.

The results of these study were published in the Journal of Atmospheric and Solar Terrestrial Physics and were part of the Master and PhD degree of Deysi Cornejo.

Instrumental Development, Installation and Operation

The 7 GHz solar polarimeter reinstallation

The 7 GHz solar polarimeter has been totally upgraded and is operating automatically on a routine basis since 2017 October at the Mackenzie University (se Figure 5)

Figure 5. 7 GHz polarimeter operating at Mackenzie University

Solar flare THz photometers on long duration stratospheric balloon flight (SOLAR-T)

The SOLAR-T (Figure 6) mission composed of a double 3 and 7 THz photometers flew on a stratospheric balloon over Antarctica together with University of California Berkeley, SSL, GRIPS experiment.

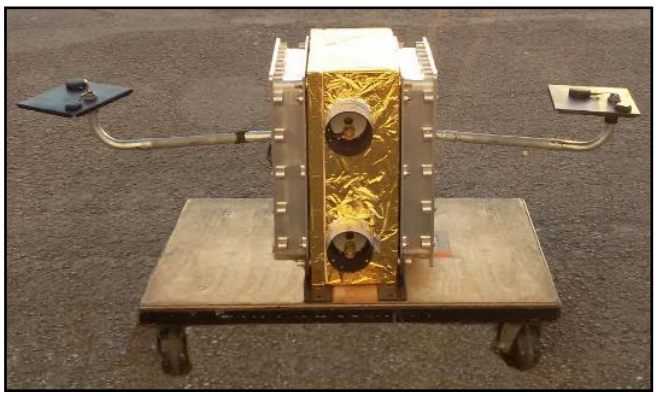

Figure 6. SOLAR-T experiment

The main result of the 16-days flight was to obtain the quiet Sun brightness temperatures at 3 and 7 THz, with values of 4800 and 4700 K, respectively.

The quiet Sun brightness temperature spectrum, recompiled from many measurements, including the SOLAR-T measurements indicates infrared emitting sources located at the minimum temperature region (see Figure 7).

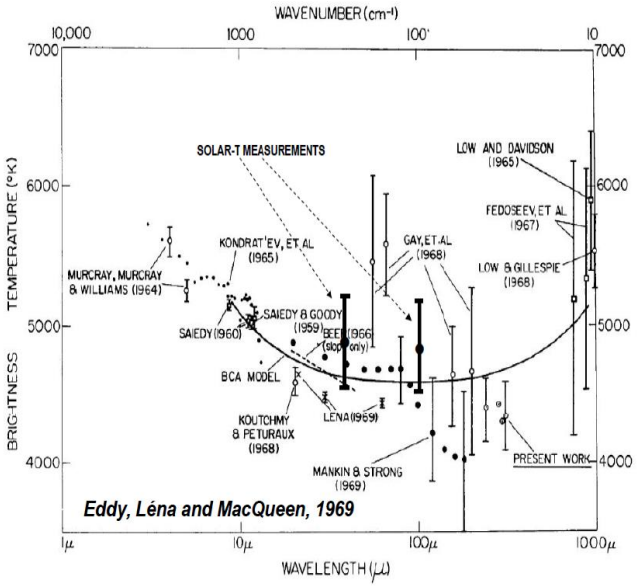

Figure 7. Quiet Sun brightness temperature spectrum, including values obtained by SOLAR-T at 3 and 7 THz.

The overall results of the SOLAR-T experiment demonstrate that 3 and 7 THz photometers were responding well and were properly calibrated and observed brightness temperatures agree well with other independent measures.

Routine observations at 30 THz (10 microns) in Argentina and Brazil

During this project two systems operating at 30 THz (10 microns) were installed in Brazil (CRAAM, UPM) and Argentina (OAFA, San Juan). Routine observations include few solar maps when atmospheric conditions allow it, as well as the definition of a dark frame, automatic calibration procedures against the quiet Sun and against the sky level, automatic limb finding and adjustment of a solar disk. Figure 8 below shows the installation in Argentina coupled to the H-alpha telescope HASTA.

Figure 8. 30 THz observing facility installed at OAFA (Argentina), coupled with H-alpha telescope.

Few solar events were observed by both instrumental facilities and will be described later in this report.

The project HATS

The High Altitude Terahertz Solar telescope has been delayed for ~ a year. The main reasons for that: (i) the loss of Pierre Kaufmann, former PI of the project; (ii) a bad initial choice for the place of installation at Famatina (5000 masl). .

Reason (ii) was the most serious, with basically no infrastructure at all, and many interaction problems with local communities.

For this reason, a decision made for a first assembly of the 16 THz version at OAFA where infrastructure, communications etc .. already exist. Specific infrastructure tasks were achieved, as a radome for wind protection, concrete base for mount. Table below gives the principal characteristics of HATS telescope.

Characteristics	Description
Frequency	16 THz
Mount	Equatorial, Paramount ME II
Óptic	f/2, aperture Ø 46 cm, rough mirror.
Where	OAFA, 2348 m.s.n.m.
Local infrastructure	Power, Internet Com., protected and closed area.
Operating mode	Assisted

HATS is in its subsystem's integration and assembly at Mackenzie University. Data acquisition and structure is being developed for final tests, integration and transportation to OAFA in the 2nd semester of 2019. We expect an installation and first light at 16 THz for the first trimester of 2020.

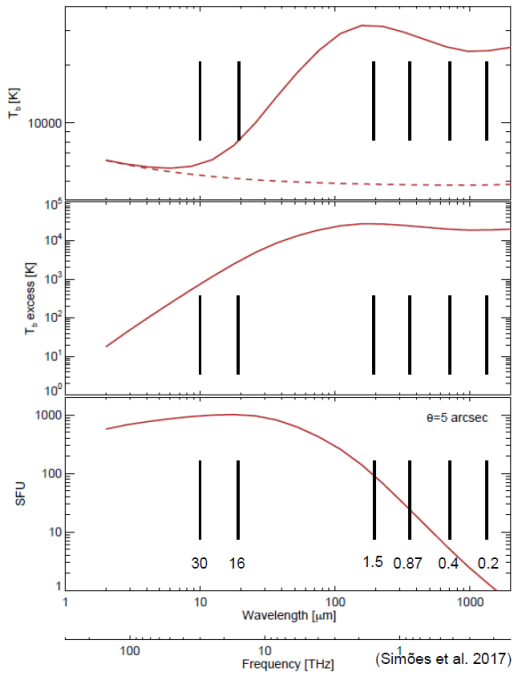

Figure 9. Expected brightness temperature in the submm and MIR/FIR range of frequencies.16 THz

Scientifically, simulations were done (Figure 9) which show that excesses of about few tens of percent of the quiet Sun brightness temperature are expected during a solar flare at this frequency of 16 THz. In Fig. 9 brightness temperature and flux density (for a 5" source size) are shown and compared with quiet Sun values.

Solar quiescent and flaring emission from GHz to THz frequencies

A new method to estimate submillimeter flux densities during solar flares

This method is based on the records at 212 and 405 GHz performed by the SST during solar scans, as shown in Figure 10.

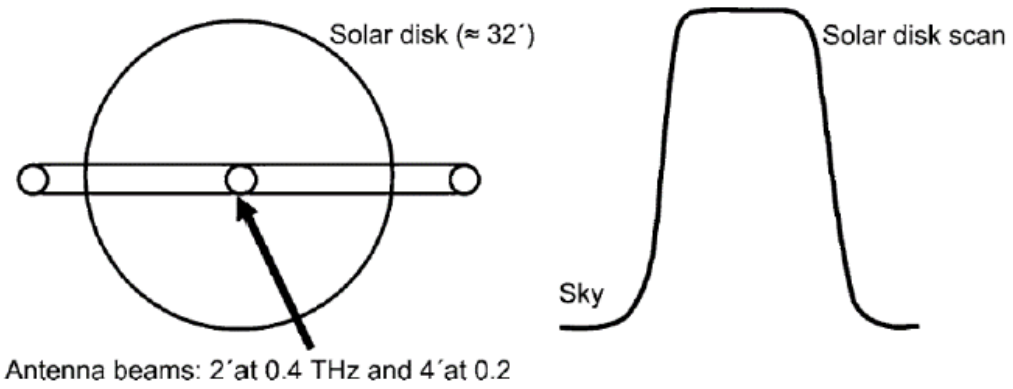

$$S = S_{\odot}(\Omega_{\text{beam}}/\Omega_{\odot}) = S_{\odot}(\theta_{\text{beam}}/\theta_{\odot})^2 \text{ SFU}$$

Figure 10. Azimuth solar scan performed by the SST. The quiet Sun level is recorded relative to the Sky emission level. Flux density scale equation obtained from the full-diak solar flux, the Sun and SST beams solid angles.

Assuming a total disk flux given in Benz (2009), and by using SST beam shapes it is possible to provide a uniform flux density scale. The importance of this method is that it is independent of any temperature calibration or atmospheric attenuation.

The spectral trend of sixteen events were studied using the SST, the 45 and 90 GHz POEMAS solar polarimeters completed by RSTN and 7 GHz polarimeter data when available between 2012 and 2016. Among the total of 16 events, 9 presented fluxes increasing with frequency above 100 GHz. The results suggest that the THz component might be present throughout, with the minimum turnover frequency increasing as a function of the energy of the emitting electrons.

These results were part of the PhD degree of Luis Olavo Fernandes, and were published in 2017 in the journal Solar Physics.

Solar radius at submillimeter wavelengths and its relation to solar activity

Solar radius was obtained from daily solar maps at 212 and 405 GHz provided by the SST for the period between 1999 and 2017. Figure 12 shows the normalized distributions at 212 GHz (left) and 405 GHz (right) of the solar radius.

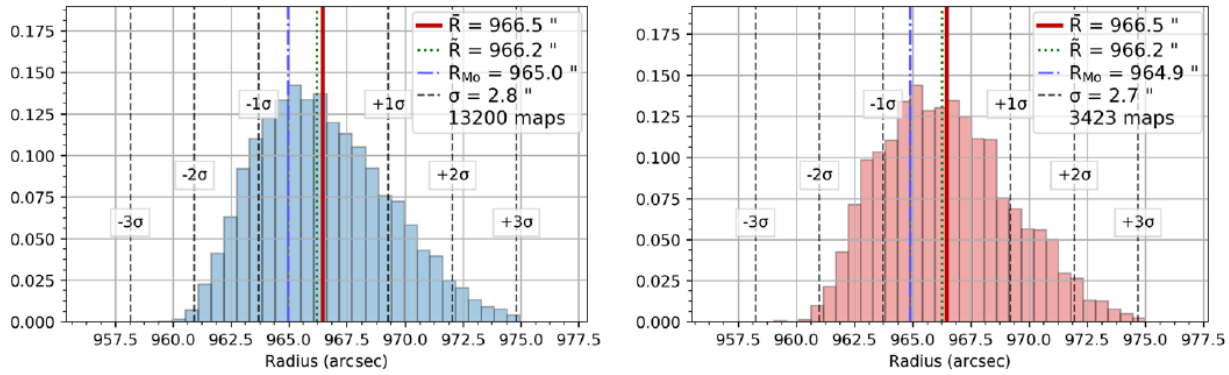

Figure 12. Radius distribution from all SST maps at 212 GHz (left) and 405 GHz (right).

Almost 17000 maps were performed at submillimeter wavelengths, and radii observed were 966.5 +/- 2.8 arcsec and 966.5 +/- 2.7 arcsec at 212 and 405 GHz, respectively. These radii locate the submm emission at an altitude above the photosphere of ~ 2000 km.

Finally, a strong anti-correlation was found for the time variability of the solar radius at submillimeter wavelengths with the solar activity cycle.

Such results indicate important information for the structure of the lower solar chromosphere. The obtained radii are similar at both frequencies which suggest that minimum value should be obtained somewhere in the submm-FIR range.

These results are part of the Master degree of Fabian Menezes, and were published in the journal Solar Physics.

Center-to-limb variation of solar bursts polarization at millimeter wavelengths and structure of the millimeter emitting sources

Polarization of radio emission from solar flares provides essential information about plasma regimes confined in coronal magnetic fields during quiescent, pre-explosive, sudden energy release and decay phases of solar flares.

Observations of polarization are carried out continuously for the first time at two-millimeter wavelengths of 6.67 and 3.34 mm (45 and 90 GHz, respectively) by two solar radio polarimeters named POEMAS operating at El Leoncito Observatory, Argentina Andes. A total of 30 solar events were observed by the radio polarimeters, between 2012 and 2013, and were analyzed.

The degree of polarization was observed to increase and then decrease as the heliocentric angle increased. We found a weak correlation between burst flux densities and their

heliocentric angle, i.e. solar bursts with higher flux density slightly tend to occur near the limb. These results are illustrated in Figure 13.

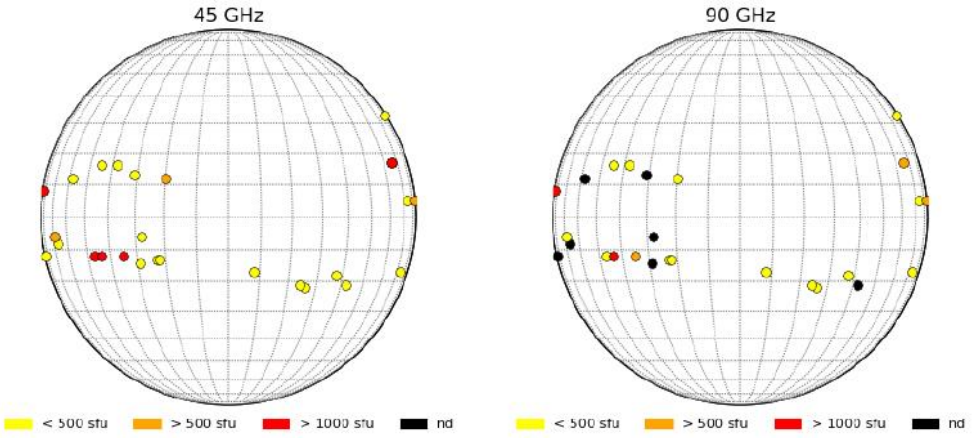

Figure 13. Relation between heliographic coordinates and intensity of solar bursts. Yellow circles represent peak flux lower than 500 s.f.u, the oranges circles represent peak flux greater than 500 and lower than 1000 s.f.u, red circles represent peak flux greater than 1000 s.f.u and black circles represent undetected bursts.

To interpret the observational results, a numerical simulation for gyro-synchrotron emission was performed. We found that the polarization degree behavior of the solar flares throughout the solar disk presents no correlation with the heliographic angle. On the other hand, the observed increasing of flux density with the heliocentric angle is predicted by the numerical simulation.

Polarization measurements are also used to investigate the magnetic field configuration, and the energy distribution of accelerated particles.

Two solar flares observed by POEMAS at 45 and 90 GHz, complemented by spectral data at microwaves from 1 - 15 GHz from the Radio Solar Telescope Network (RSTN) and at high frequencies (212 GHz) by the Solar Submillimeter Telescope (SST) were studied.

The Reuven Ramaty High-Energy Solar Spectroscopic Imager (RHESSI) hard X-ray data were used to characterize the source morphology. For each flare, we measured the source flux density at 45 and 90 GHz and the intensity of the polarization degree, that had the same polarity at both frequencies. The flux and polarization radio spectra were fitted using a model that simulates gyro synchrotron emission in an inhomogeneous 3D magnetic field loop structure. The observations were fitted by the model using the Markov Chain Monte Carlo (MCMC) method. The simulations reproduced the observed degree of polarization and radio flux spectra for each event yielding the physical parameters of the loop and flaring sources. The results indicated that the high degree of polarization during the solar explosion can be explained by two sources located at the foot points of highly asymmetric magnetic loops whereas low polarization degrees arises from foot point sources of symmetric magnetic loops. These results are illustrated in Figure 14.

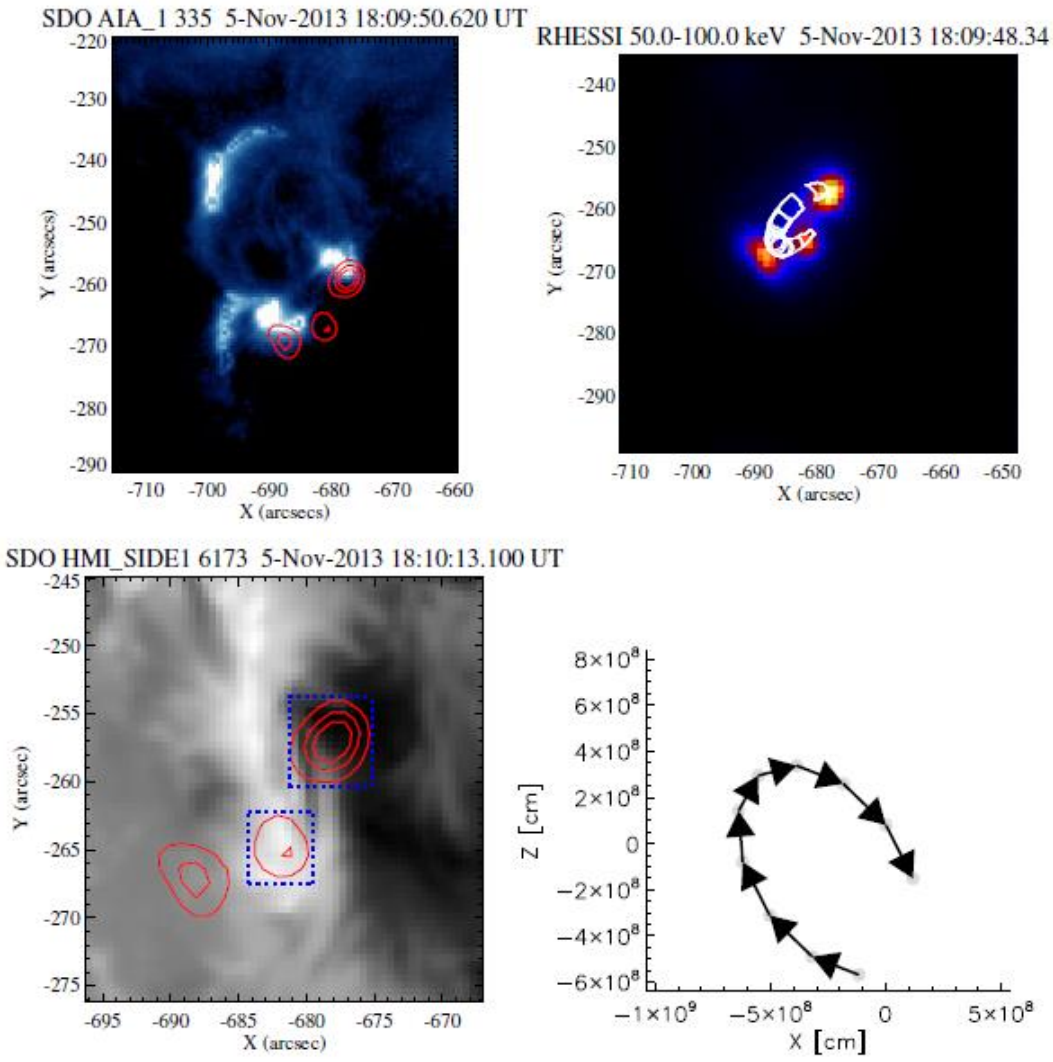

Figure 14. Top: (left) The RHESSI HRX 50 to 100 keV intensity (red) contours overlaid on an AIA 335 A image during the impulsive phase of the flare. (rigth) The modelled loop resulting from the fit overlaid on the RHESSI HRX 50 to 100 keV. Bottom: (left) magnetogram of the region with RHESSI HRX 50 to 100 keV emission (red contours); and (rigth) the polarity of the modelled magnetic field resulting of the best fit.

Part of these results were obtained by the PhD students MSc. Ray Hidalgo and MSc. Douglas Silva. Two papers were submitted to the journal Solar Physics.

Submillimeter flare emission and the Neupert effect

The event under study is the M2.2 GOES-Class flare on 2011, Feb. 14 at 17:25 UT. Figure 15 shows the time evolution of the M2.2 flare including time profiles at soft X-rays, submillimeter (212 GHz) waves, microwaves, and hard X-rays. In this plot we also include the spectral index deduce from the observed points at 15.4 GHz and 212 GHz.

The Neupert effect is an empirical relation between the time profile of non-thermal processes (e.g. hard X-rays) and the time derivative of thermal processes (e.g. soft X-rays).

In the present event, we interpret that the 212 GHz emission can be understand as the thermal component of the Neupert effect. Indeed, we find that the maximum of hard X-rays above 50 keV coincides with the time derivative of the submillimeter emission. This is suggested from the examination of Figure 16. The spectral index in the optically thin regime also indicates that the 212 GHz emission is probably from thermal origin due to the bremsstrahlung process, in the chromospheric layers at the beginning of the event, and from the hot thermal coronal plasma later.

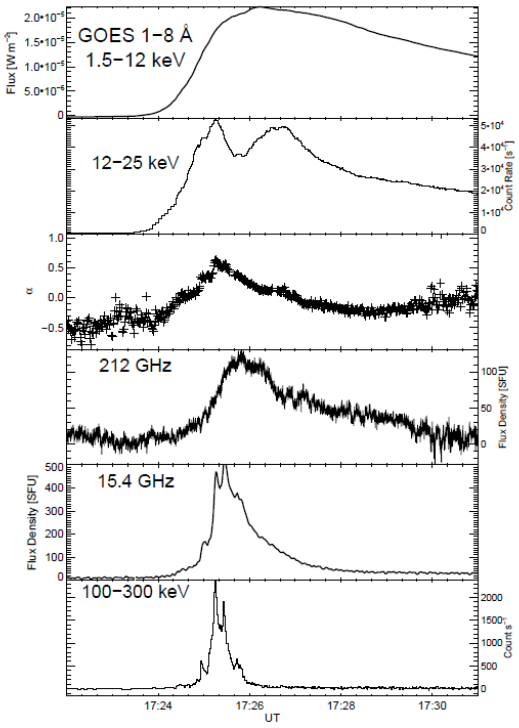

Figure 15. Time profile of the M2.2 flare on 2011, Feb. 14 at 17:25 UT. From top to bottom: (i) GOES low energy channel; (ii) Fermi GBM 12-25 keV ; (iii) 15.4 – 212 GHz spectral index; (iv) 212 GHz emission; (v) microwave 15.4 GHz emission; (vi) FERMI GBM 100-300 keV.

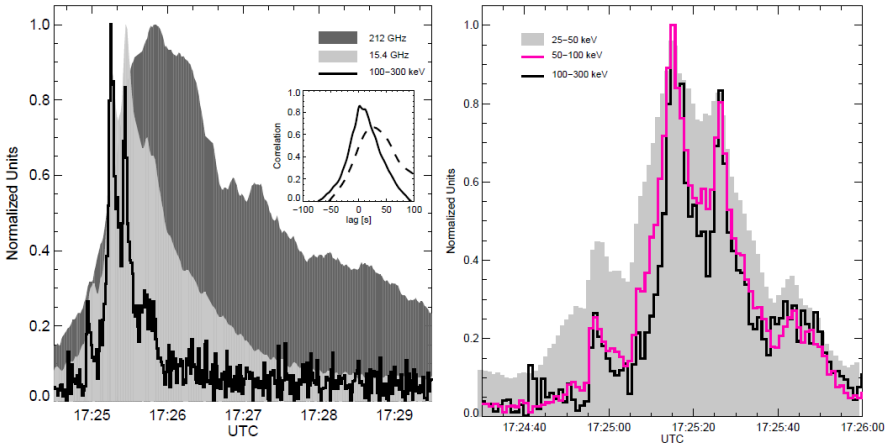

Figure 16. Left: Normalized intensities at 212 GHz (shaded dark gray), 15.4 GHz (shaded light grey) and 100-300 keV (black curve). In the inset, the cross correlation in function of the time lag between 100-300 keV and 15.4 GHz (continuous curve) and between 100-300 keV and 212 GHz (dashed curve). Right: Normalized count rates at 25-50 keV (shaded light gray), 50-100 keV (magenta curve) and 100-300 keV (black curve).

These results are part of the Post-Doc activities of Jorge Fernando Valle. A paper is submitted in the journal Astronomy & Astrophysics.

The unusual high solar Activity in September 2017

Active Region 12673 produced the most intense event of the solar cycle 24: in a few days of early September 2017, four X-class and eight M-class flares occurred. SOL2017-09-06T12:00, a GOES X9.3 flare, that also produced a two-ribbon white-light emission across the sunspot detected by SDO/HMI, was observed at 212 and 405 GHz with the arcminute-size beams of the Solar Submillimeter Telescope focal array while making a solar map. This unique situation is illustrated in Figure 17, showing the solar map scans performed by the SST at the time of the X9.3 flare (left) as well as the reconstructed 2D map at 212 GHz (right). For this event it will be possible, in principle, to calibrate the SST output using directly the Sun temperature at 212 GHz, independently of other temperature calibration and atmospheric attenuation correction. A preliminary analysis gives 5900 and 1800 K at 212 and 405 GHz, respectively.

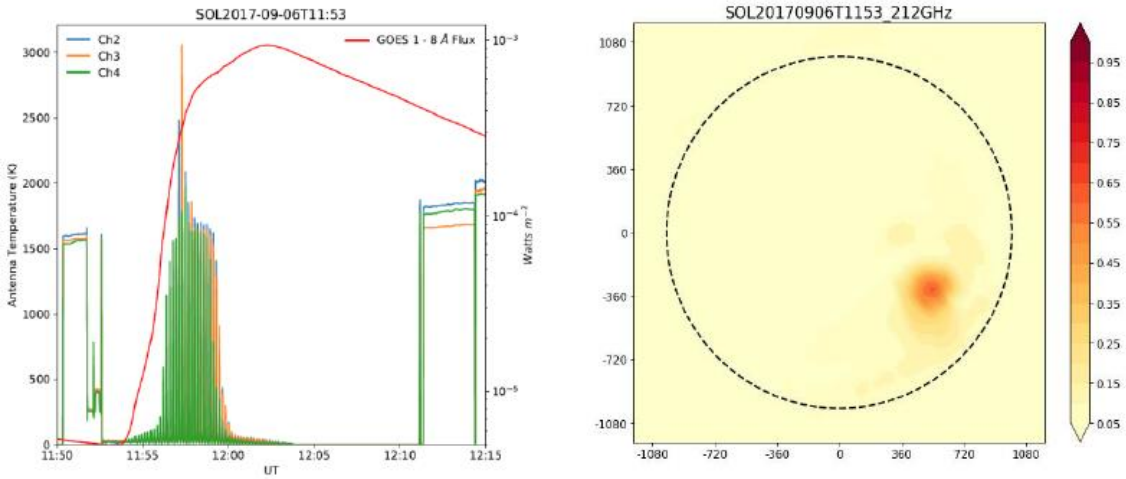

Figure 17. Left: Consecutive solar scans of the Sun at 212 GHz at the time of the flare occurrence. Right: 2D solar map at 212 GHz from azimuth solar scans. The flare emitting source is observed in the SW quadrant.

This event was also observed at 30 THz (10 μm) using the 17 arcsec diffraction limit IR camera installed at the Solar Observatory at Mackenzie University. Figure 18 below shows the overall time profile of the event.

Images at 10 microns revealed that the sunspot gradually increased in brightness while the event proceeded, reaching a temperature like quiet Sun values. From the images we derive a lower bound limit of 180-K flare peak excess brightness temperature or 7,000 sfu if we consider a similar size as the white light source. The rising phase of mid-IR and white light is similar, although the latter decays faster, and the maximum of the mid-IR and white light emission is ~ 200 s delayed from the 15.4-GHz peak occurrence. The submillimeter spectrum has a different origin than that of microwaves from 1 to 15 GHz, although it is not possible to draw a definitive conclusion about its emitting mechanism.

But more importantly is the similarity between WL and 30 THz flare emission time history as shown in Figure 18, which suggests that the possibility of 30 THz flare emission being used as proxy for WL emission deserves further investigation.

These results are part of the Post-Doc activities of Jorge Fernando Valle. A paper has been published in the journal Space Weather.

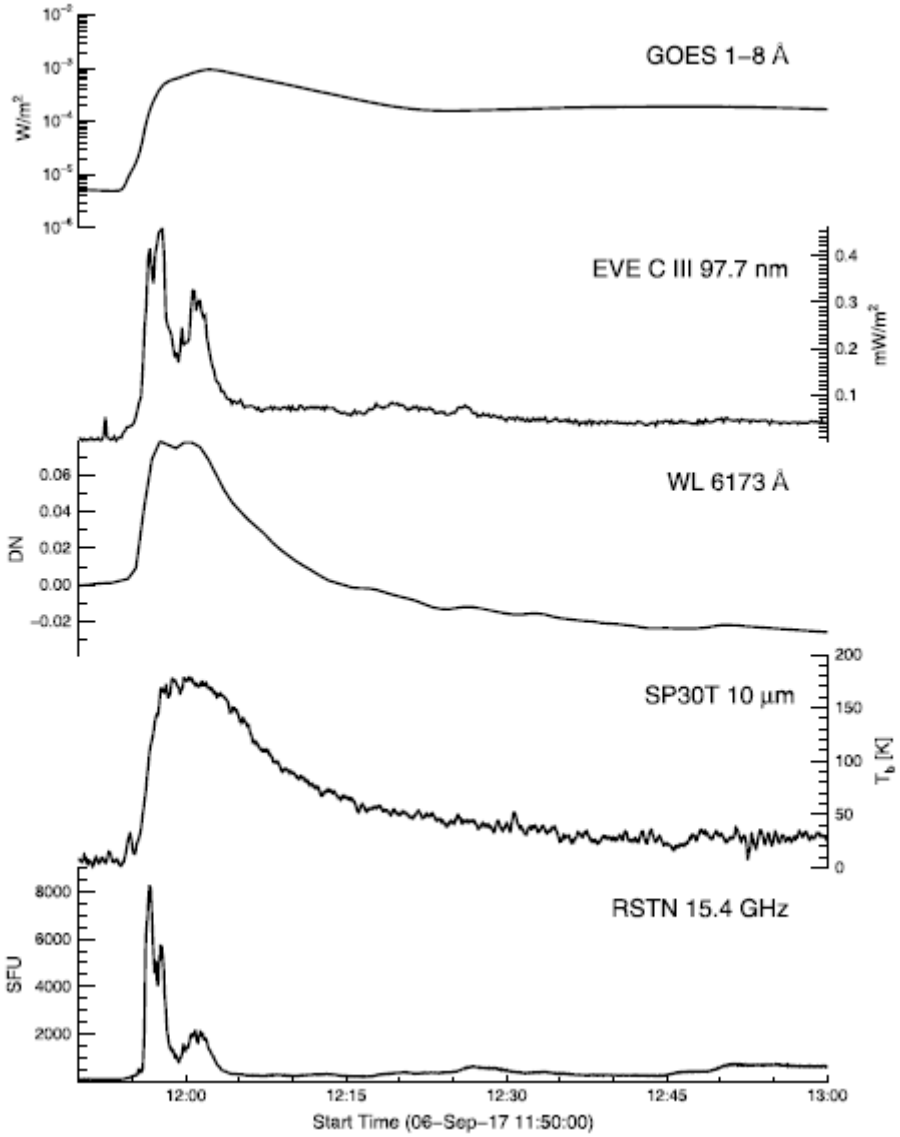

Figure 18. Intensity time profiles at selected wavelengths from GOES, EVE, WL and RSTN

Secondary e^- and e^+ during solar flares - HXR/γ-ray spectra

Nuclear processes during solar flares can result in the production of pions which decay in photons of ~ 70 MeV, and electrons and positrons in the same energy range. These secondary particles can also radiate synchrotron radiation in the coronal plasma embedded within the solar magnetic field.

For this we use the code FLUKA which considers all nuclear interactions and estimate the number of secondary particles given the energy distribution of a primary accelerated proton population. So far, such computation models were exhaustively used although (i) without considering the transport of these secondary particles, and (ii) neglecting the production of secondary (knock-on) electrons from direct ionization.

Figure 19 shows the results of a FLUKA simulations performed within the above conditions. Two differences compared to earlier results are clearly seen that are discussed below.

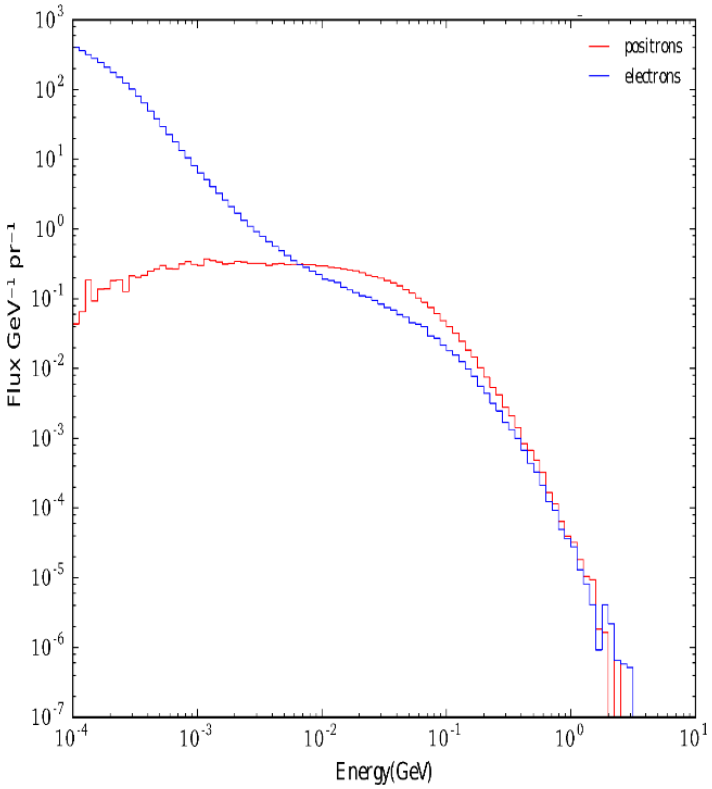

Figure 19. Secondary particles (electrons, positrons) production during solar flares which shows the effects of transport and presence of knock-on electrons.

The first difference is the presence of energetic positrons down to energies of about 100 keV. Without transport, the positron number would have decreased by about one order of magnitude between 10 MeV and 1 MeV. Therefore, these results suggest that synchrotron emission from positrons may not be negligible as was thought in the past.

The second difference is the presence of an important distribution of secondary electrons up to at least few MeV. It is due to the production of knock-on electrons produced after direct ionization of chromospheric or photospheric elements by primary protons. This distribution has never been considered in the synchrotron calculations during solar flares. If considered it probably will reduce the requirements in terms of electron number. Therefore, and as discussed in a previous partial report for the microbunching instability, the secondary electron distribution may bring new important information to understand the well-known "electron number problem", specifically during large solar flares.

The next step in these computations will be to consider an ambient magnetic field, which can be done by using the GEANT 4 numerical code.

Further progress in a tentative to have a self-consistent modelling of Hard X-ray and γ-ray spectrum were done. The main results are illustrated in Figure 20 which suggests that FLUKA simulations can provide templates for the full hard X-ray and γ-ray spectrum

including all components as nuclear de-excitation lines, 511 keV annihilation line, the 2.2 MeV capture line, and the photon continuum from pion decay.

In Figure 20 we show that a single spectrum from few hundreds keV up to few hundreds' MeV can be obtained which adjust satisfactorily well photon fluxes from both RHESSI and FERMI/LAT/GBM detectors.

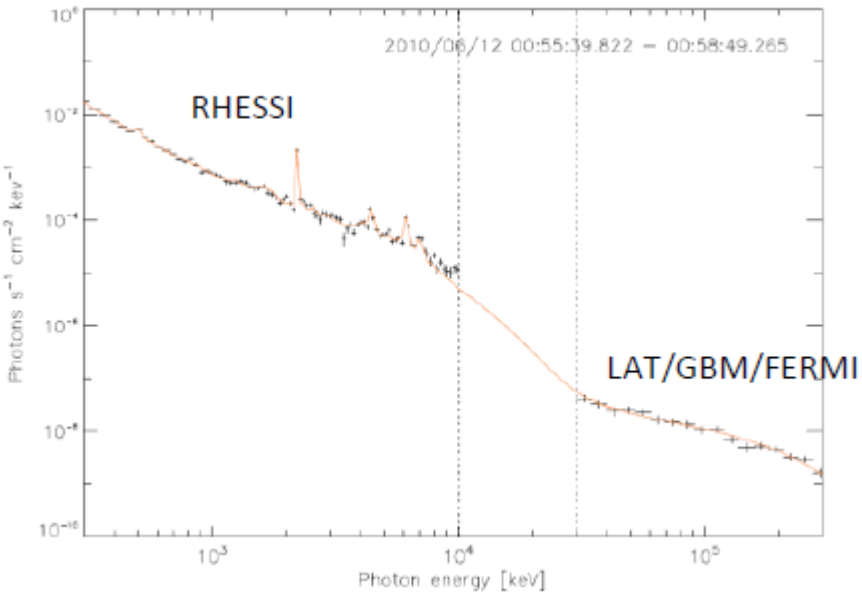

Figure 20. Comparison of secondary particles during solar flares which shows the effects of transport.

These findings are part of the PhD degree (in progress) of Jordi Tuneu and of the PhD degree (completed) of Daneele Tusnski. Three papers are submitted to the journal Solar Physics.

REFERENCES

Benz, A.O., 2009. Quiet and slowly varying solar emissions of the Sun, In: Trumper, J.E. (ed.) Landot-Bornstein – Group IV Astronomy and Astrophysics, Numerical Data and Evolutional Relationships in Science and Technology, SolAR System, **4B**, Springer, Berlin, 103.

Melo, A. M., Kaufmann, P., Giménez de Castro, C. G., Raulin, J.-P., Levato, H., Marun, A., Giuliani, J. L., Pereyra, P., 2005. Submillimeter-wave atmospheric transmission at El Leoncito, Argentina Andes, IEEE T Antenn. Propag., **53**, 1528-1534.

Kaufmann, P., Raulin, J.-P., Giménez de Castro, C. G., Levato, H., Gary, D. E., Costa, J. E. R., Marun, A., Pereyra, P., Silva, A. V. R., Correia, E., 2004. A new solar burst spectral component emitting only in the terahertz range, Astrophys. J., **603**, L121-L124.

Kaufmann, P., Raulin, J.-P., 2006. Can microbunch instability on solar flare accelerated electron beams account for bright broadband coherent synchrotron microwaves? Phys. Plasmas, **13**, 070701, doi: http://dx.doi.org/10.1063/1.2244526.

Kaufmann, P., White, S. M., Freeland, S. L., Marcon, R., Fernandes, L. O .T., Kudaka, A. S., de Souza, R. V., Aballay, J. L., Fernandez, G., Godoy, R., Marun, A., Valio, A., Raulin, J.-P., Giménez de Castro, C. G., 2013. A bright impulsive solar burst detected at 30 THz. Astrophys. J., **768**, 134-143, doi:10.1088/0004-637X/768/2/134.

Otarola, A., Hiriart, D., Perez-Leon, J.E., 2009. Statistical characterization of precipitable water vapor at San Pedro Martir Sierra in Baja California. Rev. Mex. Astron. Astrofísica **45**, 161–169.

Otarola, A., Travouillon, T., Schock, M., Els, S., Riddle, R., Skidmore, W., Dahl, R., Naylor, D., Querel, R., 2010. Thirty meter telescope site testing X: precipitable water vapor. Publ. Astron. Soc. Pac. **122**, 470–484.

Otero, L., Ristori, P., D'Elía, R., Pallotta, J., Quel, E., 2013. Study of CASLEO clear sky aerosol loads in 2011 from one year of aeronet quality assured data, in: Proceedings of the 33rd International Cosmic Ray Conference (ICRC 2013), Rio de Janeiro (Brazil).

Smirnov, A., Holben, B. N., Eck, T. F., Dubovik, O., Slutsker, I., 2000. Cloud-screening and quality control algorithms for the AERONET database, Remote Sens. Environ. 73, 337-349.

Trottet, G., Krucker, S., Luthi, T., Magun, A., 2008. RADIO SUBMILLIMETER AND γ-RAY OBSERVATIONS OF THE 2003 OCTOBER 28 SOLAR FLARE, Astrophys. J., **678**, 509-514.

Trottet, G., Raulin, J.-P., Mackinnon, A., Giménez de Castro, G., Simões, P. J. A., Cabezas, D., de La Luz, V., Luoni, M., Kaufmann, P., 2015. Origin of the 30 THz emission detected during the solar flare on 2012 March 13 at 17:20 UT, Sol. Phys., 290, 2809-2826, doi: 10.1007/s11207-015-0782-0.

SCIENTIFIC PRODUCTION

During the whole project twelve (12) papers were produced, eight (8) are published, four (4) are submitted (see list below)

- Nicoll, K.A.; Harrison, R.G.; Barta, V.; Tacza, J.; Raulin, J.-P. et al. "A global atmospheric monitoring network for climate and geophysical research". *Journal of Atmospheric and Solar-Terrestrial Physics*, **184**, 18-29, 2019.
- Valle Silva, J.F.; Giménez de Castro, C.G.; Selhorst, C.L.; White, S.M.; Raulin, J.-P.; Valio, A., "Spectral Signature of Solar Active Region from Centimeter to Submillimeter Wavelengths", *Solar Physics*, submitted, 2019
- Valle Silva, J.F.; Giménez de Castro, C.G.; Simões, P.J.A.; Raulin, J.-P., "Submillimeter radiation as the thermal component of the Newpert effect", *Solar Physics*, submitted, 2019
- Da Silva, D.F.; Simões, P.J.A.; Hidalgo Ramirez, R.F.; Valio, A., "Magnetic field asymmetry and the degree of polarization at millimeter wavelengths of solar flares", *Solar Physics*, submitted, 2019
- Hidalgo Ramirez, R.F.; Morosi, A.; Da Silva, D.F.; Simões, P.J.A.; Valio, A., "Center-to-limb variation of solar bursts polarization at millimeter wavelengths", *Solar Physics*, submitted, 2019
- Cassiano, M.M.; Cornejo Espinoza, D.; Raulin, J.-P.; Giménez de Castro, C.G. "Precipitable water vapor and 212 GHz atmospheric optical depth correlation at El Leoncito site". *Journal of Atmospheric and Solar-Terrestrial Physics*, **168**, 32-36, 2018
- Giménez de Castro, C.G.; Raulin, J.-P.; Valle Silva, J.F.; Kudaka, A.S.; Valio, A.B.M. "The September 6, 2017 X9 super flare observed from submillimeter to Mid-IR" *Space Weather International Journal of Research and Applications*, **16**, 1261-1268, 2018

- Menezes, F.; Silva, A., "Erratum: Correction to: Solar Radius at Subterahertz Frequencies and Its Relation to Solar Activity", *Solar Physics*, **293**(6), 1pp., 2018
- Fernandes, L.O.T.; Kaufmann, P.; Correia, E.; Giménez de Castro, C.G.; Kudaka, A.S.; Marun, A.; Pereyra, P.; Raulin, J.-P.; Valio, A. "Spectral Trends of Solar Bursts at Sub-THz Frequencies". *Solar Physics*, **292**(21), 12pp., 2017.
- Penn, M.; Krucker, S.; Hudson, H.; Jhabvala, M.; Jennings, D.; Lunsford, A.; Kaufmann, P. "Spectral and Imaging Observations of a White-Light Solar Flare in the Mid-Infrared". *Astrophysical Journal Letters*, **819**(L30), 5pp, 2016. DOI: 10.3847/2041-8205/819/2/L30.
- Menezes, F.; Silva, A., "Solar Radius at Subterahertz Frequencies and Its Relation to Solar Activity", *Solar Physics*, **292**(12), 10pp., 2017
- Miteva, R.; Kaufmann, P.; Cabezas, D.P.; Cassiano, M.M.; Fernandes, L.O.T.; Freeland, S.L.; Karlický, M.; Kerdraon, A.; Kudaka, A.S.; Luoni, M.L.; Marcon, R.; Raulin, J.-P.; Trottet, G.; White, S.M. "Comparison of 30 THz impulsive burst time development to microwave, Há, EUV, and GOES soft X-rays*". Astronomy & Astrophysics*, **586**, idA91, 4pp, 2016. DOI: 10.1051/0004-6361/201425520.
- Giménez de Castro, C.G.; Simões, P.J.A.; Raulin, J-P.; Guimarães Jr, O.M. "Analysis of intermitency in submillimeter radio and Hard X-Rays during the impulsive phase of a solar flare". *Solar Physics*, **291**(7), pp. 2003-2016, 2016. DOI: 10.1007/s11207-016-0949-3.

In addition to the papers listed above, there were seven (7) papers published in conference proceedings, twelve (12) invited talks in international conferences, twenty-two (22) abstracts in international conferences, and thirteen (13) abstracts in Brazilian conferences.

HUMAN RESOURCES

During the project three (3) students received their PhD and one (1) student received her Master.

At this time four (4) PhD students are involved, and three (3) of them will get their degree in 2019.

Finally, two (2) post-doc participated to the project

HIGHLIGHTS

- Institutional Mackenzie University Support: hiring one project manager and one chief-engineer

- Jean-Pierre Raulin: award for the 2018 highest scientific production at Mackenzie University